A 2-D Magnetotelluric Investigation of the Cascadia Subduction Zone

by

Nicholas Wogan

A THESIS

Presented to the Department of Physics
and the Robert D. Clark Honors College
in partial fulfillment of the requirements for the degree of
Bachelor of Science

June, 2016

An Abstract of the Thesis of

Nicholas Wogan for the degree of Bachelor of Science
in the Department of Physics to be taken June, 2016

Title: A 2-D Magnetotelluric Investigation of the Cascadia Subduction Zone

Approved: 

Dean Livelybrooks

I have produced four 2-D magnetotelluric conductivity inversions of MOCHA data roughly between the latitudes of 43N and 46N that indicate fluid variation along strike in the Cascadia subduction zone. I directly compare these results to Wannamaker et al. 2014 EMSLAB inversion and find the models to be very similar despite the use of different data sets and inversion methods. Conductivity structure along the plate interface supports the hypothesis that there is "partial creeping" occurring in the locked zone in central Cascadia, as well as the possible presence of a secondary, inboard locked zone at 44.5N in the ETS region. The variability of conductivity along strike also suggests a more permeable crust in the northern region of Cascadia directly overhead the ETS zone, and more fluid accumulation in this same region. This study indicates that a more permeable overlying crust, combined with larger amounts of fluid present may be critical components of rapid ETS occurrence.

Acknowledgements

I need to thank my thesis advisor, Professor Dean Livelybrooks, and second reader, Blake Paris, for all of the help and guidance that they have provided me. I could not have chosen better mentors. I need to also thank Professor Eugene Humphreys for providing me with guidance towards the end of the project. Thanks to the rest of the Livelybrooks Group, Max Kant, Alexa Zeryck, Michael Skidmore, Alex Cook, and Anna Cohen, for helping me troubleshoot Matlab code, construct figures, and helping edit this paper. Credit for this this research can be attributed to all of the Livelybrooks Group.

Table of Contents

List of Figures

Introduction

A subduction zone marks a collision between two of Earth's tectonic plates. Figure 1 depicts the Cascade subduction zone where an oceanic plate dives slowly beneath a less dense continental plate into the mantle of the earth. There are many subduction zones in the world, all of which build up stress between tectonic plates over hundreds of years, then release this energy periodically in the form of earthquakes.[1] Full-scale subduction zone earthquakes, known as megathrust events, are the world's largest earthquakes.

The 2011 Tohoku Earthquake is the most recent example of a great megathrust event. The Tohoku subduction zone is composed of the overriding Eurasian plate and the subducting Pacific plate. On March 11, 2011 the Eurasian plate slipped 300 km along strike and produced a M 9.0 earthquake in addition to a tsunami that reached heights of 29 meters.[2] The 2004 Indian Ocean Tsunami was the result of another well-known M 9.1 megathrust. This resulted from the Indian plate slipping or subducting under the Burma plate. The resulting tsunami reached heights of up to 30 meters, which caused 230,000 deaths among 14 countries making it one of the most deadly natural disasters in history.[3] Geophysical studies of subduction zones are of academic interest, but more importantly may yield a better understanding of the rapid evolution of megathrust earthquake events and their future impacts on society.

---

[1] Stern, https://www.utdallas.edu/scimathed/resources/Melville/g_wherearesubductionzones.html.
[2] "The Watchers" , http://thewatchers.adorraeli.com/2011/12/04/we-watch-is-japan-going-to-sink-pt-3-seabed-shifted-by-50-meters165-feet-the-largest-slip-yet-recorded/.
[3] https://en.wikipedia.org/wiki/2004_Indian_Ocean_earthquake_and_tsunami#Earthquake_characteristics

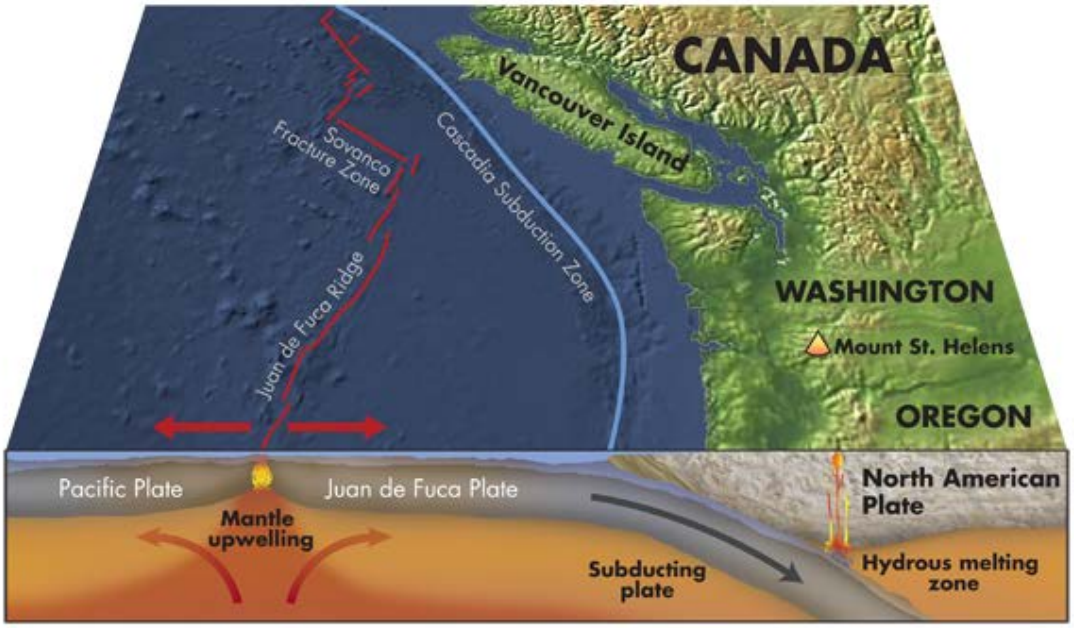

Figure 1. The Cascadia subduction zone.[4]

New oceanic plate is formed at offshore ridges and progresses eastward relative to the North American plate. The oceanic plate thrusts below the North American plate at the 'trench' (blue line), beginning the subduction process. Fluids that are carried down with the subducted plate, undergo various pressure- and temperature-driven reactions that either incorporate them in metamorphic minerals or exsolve them, typically into the interface zone. The presence of the fluids in the mantle underlying the North American Plate serves to flux melting reactions, creating magmas that rise to form the volcanoes of the Cascades Range.

Closer to home is the Cascadia subduction zone which extends from Northern California through British Columbia. The Juan de Fuca plate is slowly subducting under the North American plate; it has been building stress in its locked zone for over three hundred years. More precisely, the two plates have been locked and building stress since 1700. This earthquake, determined to be a 9.0 on the Richter scale, was the last large subduction earthquake in the Cascadia region. This date was determined from

[4] http://www.earthmagazine.org/article/unlocking-cascadia-subduction-zones-secrets-peering-recent-research-and-findings.

Japanese tsunami records and confirmed by seismologists at the University of Washington. Scientists also analyzed Native American stories of a great earthquake that happened roughly seven generations ago. After analyzing core samples of the seafloor, Goldfinger et al. at Oregon State University was able to determine that there have been forty-one subduction zone earthquakes in the past ten thousand years; On average, these earthquakes occur every two hundred and forty three years. It has been three-hundred-and-fifteen years since such an event.[5]

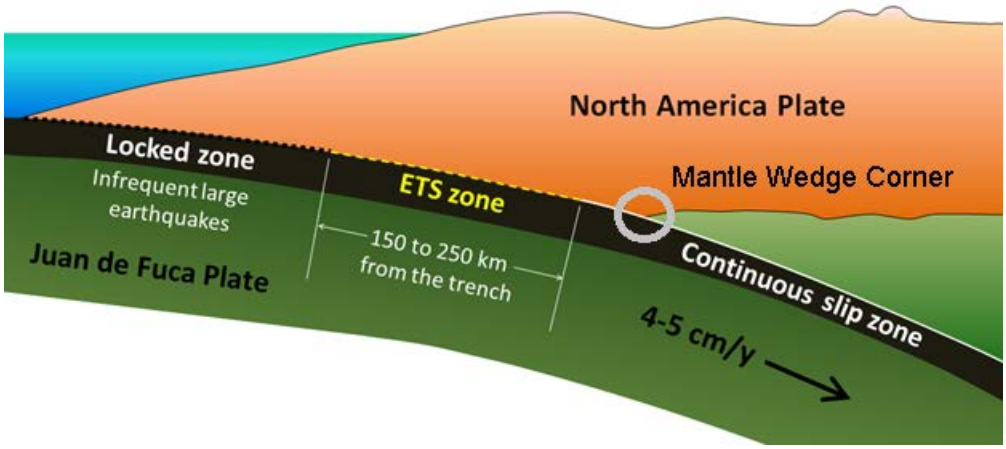

Figure 2: A subduction zone in more detail.

Note the ETS zone is located in between the locked zone and the free slip zone.

The locked zone, ETS (episodic tremor and slip) zone, and continuous slip zone nominally underlying the mantle wedge corner, are regions of interest when studying a subduction zone (Figure 2). The mantle wedge corner is the most up-dip portion of the mantle that sits on top of a subducting plate (grey circle in Figure 2). The ETS zone is located in between the locked zone and the continuous slip zone at the mantle wedge corner. The locked zone is the region of a subduction zone that locks and slowly builds stress as the underlying plate subducts. Once the frictional strength between the plate is

[5] Shulz, 2015

overcome by the stress of subduction, the plate violently slips and generates a megathrust event. The plates slowly but consistently grind against each other in the continuous slip zone (below ETS). The "slow slip" zone or ETS zone is what bridges the gap between the locked zone and the continuous slip zone.[6] ETS is an earthquake produced from two plates slipping very slowly after locking for a short period of time, hence the name episodic tremor and slip. It is thought that an ETS earthquake has the potential to catalyze the occurrence of a megathrust event. The small scale slip during an ETS event could translate just enough stress up-dip to trigger a large scale slip (megathrust) in the locked zone.[7]

The location of fluids and zones of permeability of the overlying crust are believed to have significant effects on the locked and ETS zones. Elevated fluid pressure in the locked zone may indicate low level of locking between the plates, which is a fundamental indicator for the extent and magnitude of a slip event along a subduction zone.[8] In addition, fluid along the plate interface in the ETS zone is believed to reduce normal stresses in the plates and thus be a critical factor for occurrence of periodic slow slip events.

I have produced four 2-D magnetotelluric conductivity inversions of MOCHA data roughly between the latitudes of 43N and 46N that indicate fluid variation along strike. I directly compare L-line inversion of MOCHA data to Wannamaker et al. 2014 EMSLAB inversion (for reference see Figure 5), and find the models to be very similar despite the use of different data sets and inversion methods. This serves to provide some

[6] Vidale, Houston, 2012
[7] Vidale, Houston, 2012
[8] Moreno et al., 2014

level of validation extensible to the other 2-D MOCHA MT lines considered here. Despite this validation, many of the features need to be further explored, ideally with 3-D inversion techniques. Conductivity structure along the plate interface supports the hypothesis that there is “partial creeping” occurring in the locked zone in central Oregon, as well as the possible presence of a secondary, inboard locked zone at 44.5N in the ETS region.[9] The variability of conductivity along strike also suggests a more permeable crust in the northern region of Cascadia directly overhead the ETS zone, and thus more fluid accumulation in this same region. This more permeable overlying crust, combined with larger amounts of fluid present may be critical components of rapid ETS occurrence.

[9] Krogstad, Schmidt, Weldon, Burgette, 2016

Geology of the Cascadia Subduction Zone

The Juan De Fuca is the last remnant of the Farallon plate that continues to subduct below the North American Plate. There are two smaller subducting remnant sub-plates that straddle the Juan De Fuca: Explorer to the north and Gorda to the south. The northern border of the subduction zone is the Queen Charlotte triple junction located just northwest of Vancouver Island, and the Mendocino Triple Junction is the southern border. The simple subduction zone model consisting of one plate overriding another subducting plate does not sufficiently describe the complexity of the Cascadia subduction zone. The subduction zone has two segmentation boundaries that run along dip (roughly east-west) at latitudes of 43, and 46 degrees north, or roughly at Oregon's northern border and the southern terminus of the Willamette Valley.[10] GPS, topographic, rock structure, and seismic evidence support this, nominally latitudinal model for segmentation.[11] This segmentation characterizes three distinct zones in Cascadia: the northern (Washington and southern British Columbia), middle (Oregon), and southern (Northern California). These three portions of Cascadia have distinct interplate locked and ETS zones, and thus distinct ways of propagating stress along dip to different locations on the plate interface.

[10] Porritt, Allen, Boyarko, Brudzinski, 2011
[11] Porritt, Allen, Boyarko, Brudzinski, 2011

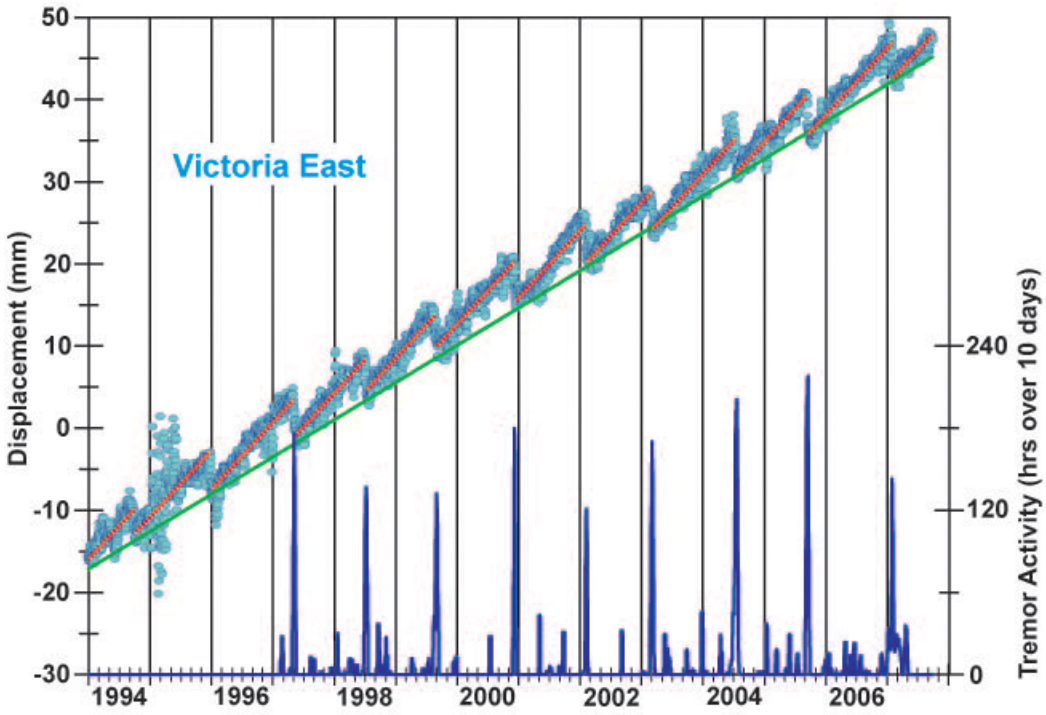

Figure 3: Seismometer and GPS data in Victoria, BC.

The data points in light blue shown is GPS data. “up” on the vertical axis corresponds to east, while “down” corresponds to west. The data in dark blue is seismometer array data indicating occurrence of tremor. The red line shows the eastern displacement over time of the North American plate in between slow slip events, while the green line indicates the average eastward motion including events. Notice that for a period of roughly 14 months, Victoria slowly moves to the east but then jumps to the west in a much shorter period of time. These jumps to the west, corresponding with tremor swarms, indicate ETS events, sometimes called ‘slow slip’ earthquakes. The slow eastward movement is the Juan de Fuca slowly pushing the North American Plate to the East. About every 14 months, there is a slow slip earthquake, and the North American Plate slips to the west.

Recall that ETS events are slow slip earthquakes that occur down-dip of the seismogenic zone after a several-month period of quiescence. ETS can be thought of as the almost undetectable earthquakes in subduction zones that happen many times, episodically, between large subduction zone events. It is thought that aqueous fluid released by the subducting tectonic plate must be present for ETS to occur. The

subducting oceanic crust contains hydrous minerals which undergo metamorphic, dehydration reactions and thus release aqueous fluids when they reach high temperatures and pressures. It is thought that the aqueous fluids travel upward and accumulate at the mantle wedge corner and along the plate interface (or ETS zone indicated in Figure 2). The fluid becomes pressurized and eventually induces cracks in the surrounding rock (tremor), including along the plate interface. The pressurized fluid lying at the interface reduces the normal stress at the plate interface which allows the plates to slip coincident with the occurrence of tremor. It is thought that the slow slip event ends when the normal forces between plates are increased by loss in fluid pressure.

It is debatable what causes the episodic increase and decrease in fluid pressure, but it is generally thought that there several factors involved. One model suggests variable pressure is induced by continuous dehydration (ecologization) and hydration (serpentinization) of minerals at the plate interface, and also the permeability of the overlying crust.[12] More permeable crusts, and larger amounts of hydrous minerals might promote more frequent ETS occurrence, the latter encouraging more frequent diffusion of fluid pressure into the overlying lithosphere, where less permeable overlying crust, and less hydrous minerals would maintain high fluid pressures for longer periods of time.[13] In summary, ETS is thought to be related to both accumulation of fluids and episodic fluctuations in fluid pressure at the plate interface, yet the specific mechanism for this episodic behavior is debatable.

[12] Audet, Bostock, Boyarko, Brudzinski, Allen, 2010
[13] Schmalzle, Mccaffrey, Creager, 2014

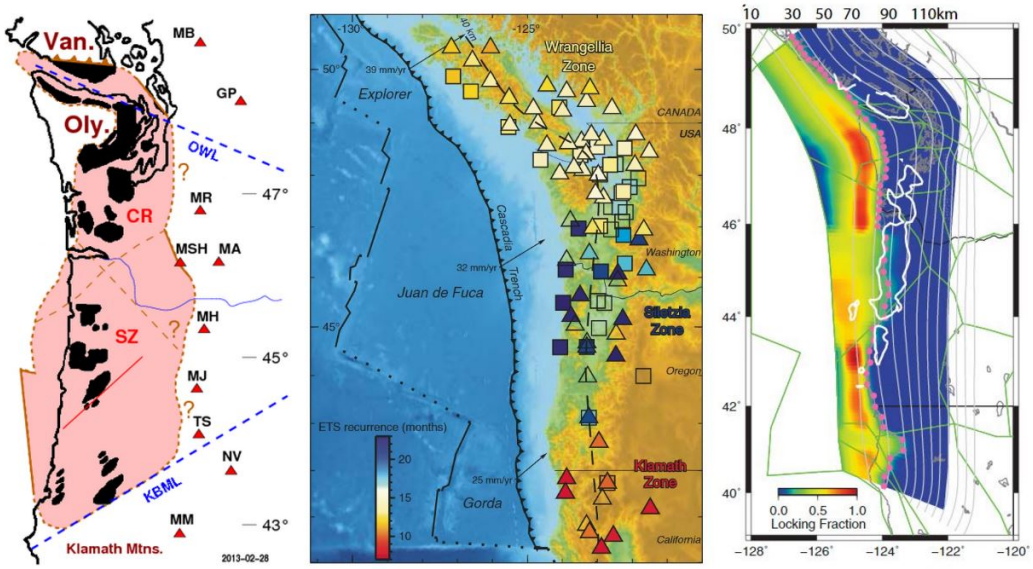

Figure 4. Siletzia, ETS and degree of Locking in Cascaida.

Left shows the Crescent (CR) and Siletzia (SZ) segments, where black indicates outcropping of underlying rock formations (pink). Red triangles indicate Cascades volcanoes. Center shows the ETS periodicity in Cascadia.[14] Red indicates higher frequency, and blue indicates lower frequency ETS. The image on the right indicates degree of locking.[15] High degrees of locking is in red, lower is yellow, and the pink dotted line indicates the eastward extent of locking. The white lines indicate gravitational anomalies.

ETS-slow slip happen at all latitudes in Cascadia, but do not have the same quasi-periodicity in each region. Slow slip events happen approximately once every 11 months in Northern California, 19 months in central Cascadia, and 14 months in southern British Columbia and northern Washington (Figure 4).[16] The borders between these regions correspond with the southern terminus of the Siletzia Terrain and the border between the Siletzia terrain and Crescent terrain shown in Figure 4. These three

[14] Brudzinski, Allen, 2007
[15] Schmalzle, Mccaffrey, Creager, 2014
[16] Brudzinski, Allen, 2007

terranes are thought to exhibit different average permeability such that the south is most permeable, the Crescent terrain is less permeable, and Siletzia is the least permeable. Notice that reduced crustal permeability seems to correspond to less frequent ETS, and higher crustal permeability to more frequent ETS. There are probably many factors controlling ETS variation, but there is evidence that it is tied to fluid content in the ETS region, and the permeability of the overlying crust. [17] [18] [19] [20]

The stress released during ETS events does not exit the subduction zone; instead it translates up-dip to the locked zone, further west. Like the variations of ETS occurrence between Cascadia's three segmentation zones, there is also variation between them in the degree of locking. GPS studies of margin-related crustal deformation indicate the central region of Cascadia has less continental uplift compared to the northern and southern regions, suggesting stronger locking in the northern and southern regions, with weak locking in the central region that undergoes "partial creeping." A subduction zone with partial creeping might evince small scale aseismic slipping in the locked zone in between major megathrust events, and also will have less pronounced slow slip.[21]

Cascadia's central region (between 43 and 46 latitudes) is shown, through GPS observations of overlying plate movement, to have a weakly locked seismogenic zone with consistent partial creeping, but it is still not clear what is responsible for the

[17] Brudzinski, Allen, 2007
[18] Furukawa, 2009
[19] Schmalzle, Mccaffrey, Creager, 2014
[20] Audet, Bostock, Boyarko, Brudzinski, Allen, 2010
[21] Audet, Bostock, Boyarko, Brudzinski, Allen, 2010

reduction in plate locking.[22] There are several theories about what is responsible for strong or weak plate locking including along-strike changes in frictional shear strength [23] [24] , geometric features of the plate interface [25], and long term slip history at the plate interface.[26] Since these parameters are not well constrained at depth, their relationship to locking degree variability remains largely elusive. Pore pressure along the plate interface, in combination with the permeability of the overlying lithosphere, have been shown to be important parameters affecting the degree of locking.[27] A receiver function study of the Costa Rican subduction zone hypothesized that high pore pressure at or above the plate interface is associated with lower degrees of locking.[28] A 3-D inversion for Poisson ratio correlated low pore pressure with large co-seismic slip, and high pore pressure with small aseismic slip during the Chilean 8.8 megathrust.[29] The presence of aqueous fluids, which is required to maintain high pore pressure, can be resolved at depth using a variety of techniques, including magnetotelluric inversions.

There is strong evidence to support lower degrees of locking between the latitudes of 43N and 46N in Cascadia[30], but there is still debate where locking actually occurs. Krogstad et al. 2016 use uplift rates to model the locking location in Cascadia. In one model, they assume only one locked zone up-dip of the mantle wedge corner, and in another model they assume two locked zones located up-dip of the mantle wedge and in the ETS region. The RMS (root-mean square residual) is reduced by a

[22] Audet, Bostock, Boyarko, Brudzinski, Allen, 2010
[23] Perfettini et al., 2010
[24] Perfettini, Ampuero, 2008
[25] Song, 2003
[26] Bürgmann, 2005
[27] Moreno et al., 2014
[28] Audet, Schwartz, 2013
[29] Moreno et al., 2014
[30] Schmalzle, Mccaffrey, Creager, 2014

statistically significant amount assuming the latter model at the latitude of 44.5 (Newport), suggesting the existence of a secondary locked zone at 31 km depth.

To summarize, Cascadia is segmented into three major regions with boundaries at 43N and 46N. The Northern and Southern regions are characterized by more frequent ETS occurrence, and higher degrees of plate locking. Central Cascadia is characterized by less frequent ETS, low degrees of plate locking (partial creep), and a possible secondary locked zone in the ETS region at 44.5N -123.5W.

Introduction to Magnetotellurics and the MOCHA Dataset

In this paper, I use magnetotelluric (MT) 2-D inversions to analyze the conductivity/resistivity structure below earth's surface. Note that conductivity is the inverse of resistivity. The following section will be dedicated to explaining the basics of MT, inversion theory, and the MOCHA dataset

Magnetotellurics is a technique used to image electrical properties beneath earth's surface. Earth- penetrating electromagnetic (EM) fields of proper frequency used for MT naturally occur in two ways. EM fields with frequencies less than 1 Hz are produced by an interaction between the solar winds and earth's magnetosphere or by thermally-induced mass motions of ions interacting with the magnetosphere. Higher frequencies fields are produced by constant worldwide thunderstorm activity. Since Earth is a moderately good conductor, penetrating EM fields induce various electrical currents in Earth that in turn produce a secondary magnetic field. These secondary fields are dependent on currents below Earth, thus they are dependent on Earth's conductivity structure. A MT station will record the total electric field both horizontal directions (Ex, Ey), and the magnetic field in all three Cartesian directions (Bx, By, Bz) at Earth's surface.

With some realistic assumptions regarding the frequency of EM fields, including the assumption that the fields are plane waves, and that lower-frequency waves sound deeper into the Earth, the ratios between different components of the electric field over the magnetic field can be used to give apparent resistivity at depth. These ratios are all contained in the impedance tensor.

$$Z = \begin{bmatrix} Z_{xx} & Z_{xy} \\ Z_{yx} & Z_{yy} \end{bmatrix} \qquad Z_{ij} = \frac{E_i}{H_j} \qquad \rho = 0.2\, T\, Z^2$$

Key Magnetotelluric Equations

The impedance tensor is on the left, and the relationship between each element in the tensor to the electric and magnetic field is in the middle. Apparent resistivity in a half space is on the right.

In this analysis of the Cascadia subduction zone, the Earth is assumed to have 2-D conductivity. The along-strike direction (x-direction), which is the north/south direction in Cascadia, is assumed to have no immediate change in conductivity. Conductivity is allowed to change in the horizontal direction (east/west or y-direction) and with depth (z-direction). The 2-D assumption implies that Zxx and Zyy in the tensor are both zero, thus we are left with Zxy, the transverse electric (TE) mode, and Zyx, the transverse magnetic (TM) mode.[31]

An MT inversion is the process of creating a resistivity model of the earth's subsurface that agrees with the collected data. MARE2D, created by Kerry Key from Scripps Institute of Technology, is the 2-D MT Inversion software used here to generate 2-D inversions. Given an estimated resistivity model of Earth, MARE2D uses Maxwell's equations governing electricity and magnetism to calculate synthetic MT data at earth's surface. This synthetic data is compared to the real data, and adjustments to the generated model are made to better match the real data. New synthetic data is calculated from the adjusted model and again compared to the real data. This iterative process continues until the synthetic data calculated from the model, and the real data

[31] Vozoff, 1972

are in close agreement. A measurement of this agreement between the synthetic data and the real data is the RMS (root-mean squared residual). Higher RMS indicates less agreement and lower RMS indicates more agreement. Any data set can agree with an infinite number of resistivity models of Earth's subsurface, thus specific constraints, such as model smoothing, are also used to guide the inversion to a realistic ending model.

A resulting inversion of magnetotelluric data will attempt to show the resistivity structure of the Earth's subsurface. In general, regions of high conductivity can be interpreted as fluid-rich zones, or rock melt, and regions of low conductivity can be interpreted as zones with little interconnected fluid or rock melt. The models being produced in this study are at shallow enough depths and cold enough zones that rock melt is likely not present. Conductors thus imply the presence of fluids, and resistors imply the lack of fluids.[32] [33]

[32] Wannamaker et al., 2014
[33] Meqbel, Egbert, Wannamaker, Kelbert, Schultz, 2014

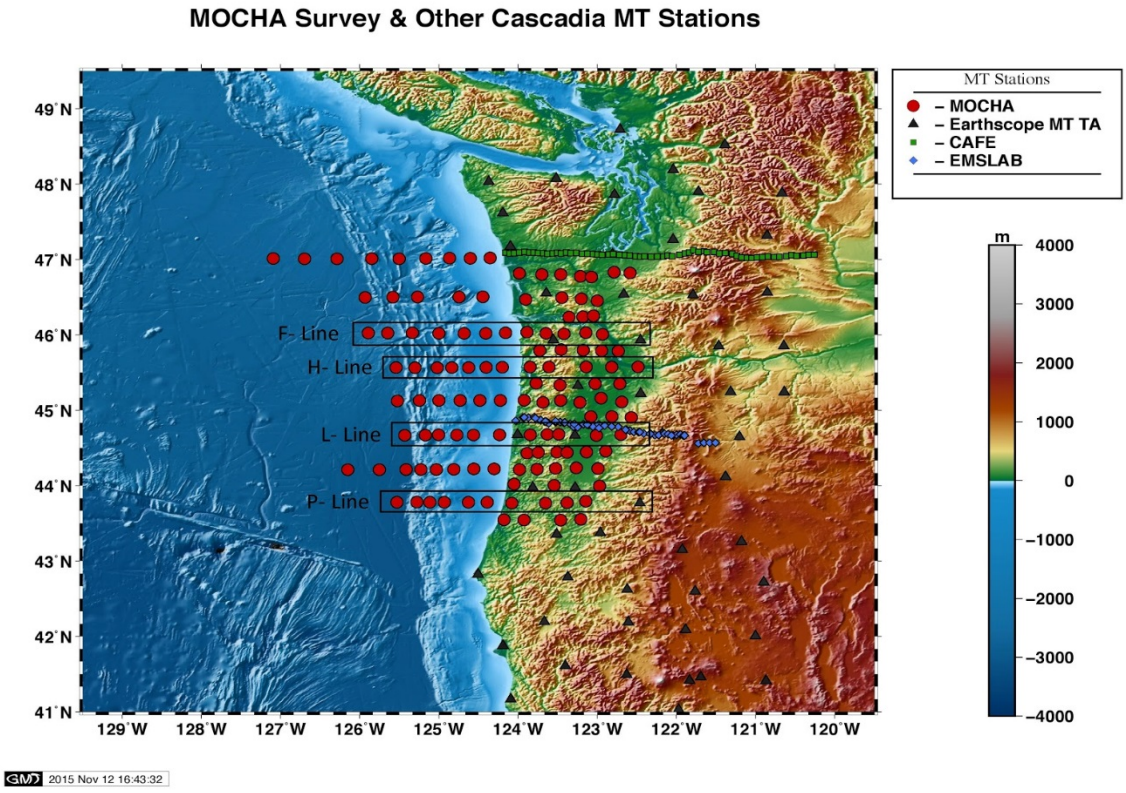

Figure 5: MOCHA, CAFE, EMSLAB, and Earthscope MT dataset.

The “lines” inverted in this study are indicated: F,H,L, and P. Image credit: Max Kant

There have been several MT surveys in Cascadia over the years but MOCHA (Magnetotelluric Observations of Cascadia using a Huge Array) is the most recent project, and is likely the first effort to acquire an array as opposed to a transect (line) of stations. Each indicated feature in Figure 5 is a MT station. MOCHA is composed from 75 land sites and 71 seafloor sites arranged in 16 horizontal lines labeled B (furthest north) through Q (furthest south) that extend from roughly 43.5° N to 47° N. The onshore data was collected from 2012-2014 and the offshore was collected April - June of 2014. The project's original intent was to analyze fluid content in the ETS zone and locked zone with 3-D inversions of the entire array. 3-D inversions are extremely

computationally intensive and have proven to take a long time to produce, so less time-consuming 2-D inversions are a useful way to initially interpret the new data. The older Earthscope, EMSLAB, and CAFE MT arrays have produced useful information on the conductivity structure of the Cascadia subduction zone. F, H, L, and P lines boxed in Figure 5 are the four lines inverted in this study, and include mostly MOCHA data, but also some Earthscope sites.

2-D MOCHA Resistivity Models

The results and interpretations of the MT transects of the MOCHA array are presented below in a format where variation along strike can be easily determined, in addition to a direct comparison between the L- line and the Wanamaker et al. 2014 interpretation of EMSLAB (ElectroMagnetic Sounding of the Lithosphere-Asthenosphere Boundary). I will first present a brief explanation of the methods and considerations made when producing these inversions using MARE2D. Next, I will discuss the inversions in detail, pointing out important features and assigning physicochemical causes or states to resistivity structure. Finally, I will make a direct comparison of principle features in L- line and EMSLAB.

The models below are inversions of TE (Ex/Hy) and TM (Ey/Hx) apparent resistivity and phase, as well as Tipper (Hz/Hy) (where x is north, y is east, and z is vertical) MOCHA data. In preparation for these final inversions the MOCHA data was adjusted and weighted using data-specific schemes to produce the most accurate 2-D inversions with a reasonable RMS. Preliminary inversions were used to manually cull data points that were clearly outliers. I was very conservative in the number of points that I culled in order to preserve the integrity of the final 2-D inversions. Weighting schemes were also applied to the data. Recall that 2-D inversions assume uniform conductivity along strike, thus, if in reality a 3-D portion of Earth was inverted using 2-D assumptions, the resulting model would display biases ascribable to fitting ranges of data reflecting 3-D structures. Although the Cascadia subduction zone can be generally characterized to have continuous resistivity structures along strike (north/south), this assumption breaks down at certain latitudes, for example where

lithological units exhibit finite latitudinal extent or where fluids vary up and down the coast. Our inversion scheme entailed using the skew as an indicator of three dimensionality to overstate TE, and TM apparent resistivity and phase errors for individual data points, thus reducing their contribution to residuals which are minimized in the MARE2D Inversion process. A similar weighting scheme was applied to the tipper.

There are two inversions shown of each 2-D cross section in Figure 6, which differ by the starting model used to produce them. Inversions in Figure 6a used a very basic starting model that only includes distinctions between the sky, sea and earth's subsurface. Earth's subsurface started at 40 ohm*m with a 500 meter deep strip of 1 ohm*m placed under the sea in order to help MARE2D deal with the large sea-earth resistivity gradient. Inversion software struggles with large, abrupt changes in conductivity, especially with stations placed on the seafloor. MARE2D attempts to minimize the misfit (RMS) between the real data and synthetic data while simultaneously maintaining smoothness. In general, conductivity structure below Earth is assumed to change relatively slowly so certain level of smoothness is required in the resulting model. The starting models used for the inversions in Figure 6b include the top of the Juan de Fuca plate.[34] This built in "slab" allows an exception to the smoothness requirement so a high conductivity gradient is allowed across the slab surface. The inversions were produced in two steps. Initial models were produced by inverting only TE and TM apparent resistivities and phases. The resulting inversion models were used

[34] Mccrory, Blair, Waldhauser, Oppenheimer, 2012

as a starting model for an inversion of TE and TM apparent resistivities and phases, and tippers.

These models are the end result of roughly one hundred different attempts, but like any inversion of any data set, they do not represent the exact conductivity structure below Earth. It is important to keep this in mind when making interpretations. Further testing of critical features needs to be done, and these lines should be compared to future 3-D interpretations of MOCHA data. There are three main things that speak to the integrity of these models: they all have a reasonably low RMS, they generally possess a conductivity structure that is geologically expected, and L- line (MOCHA data set) appears to be very similar to the Wannamaker et al. 2014 EMSLAB (EMSLAB data set). Every model was produced using the same inversion methods and parameters so this similarity speaks to the integrity of all of the inversions.

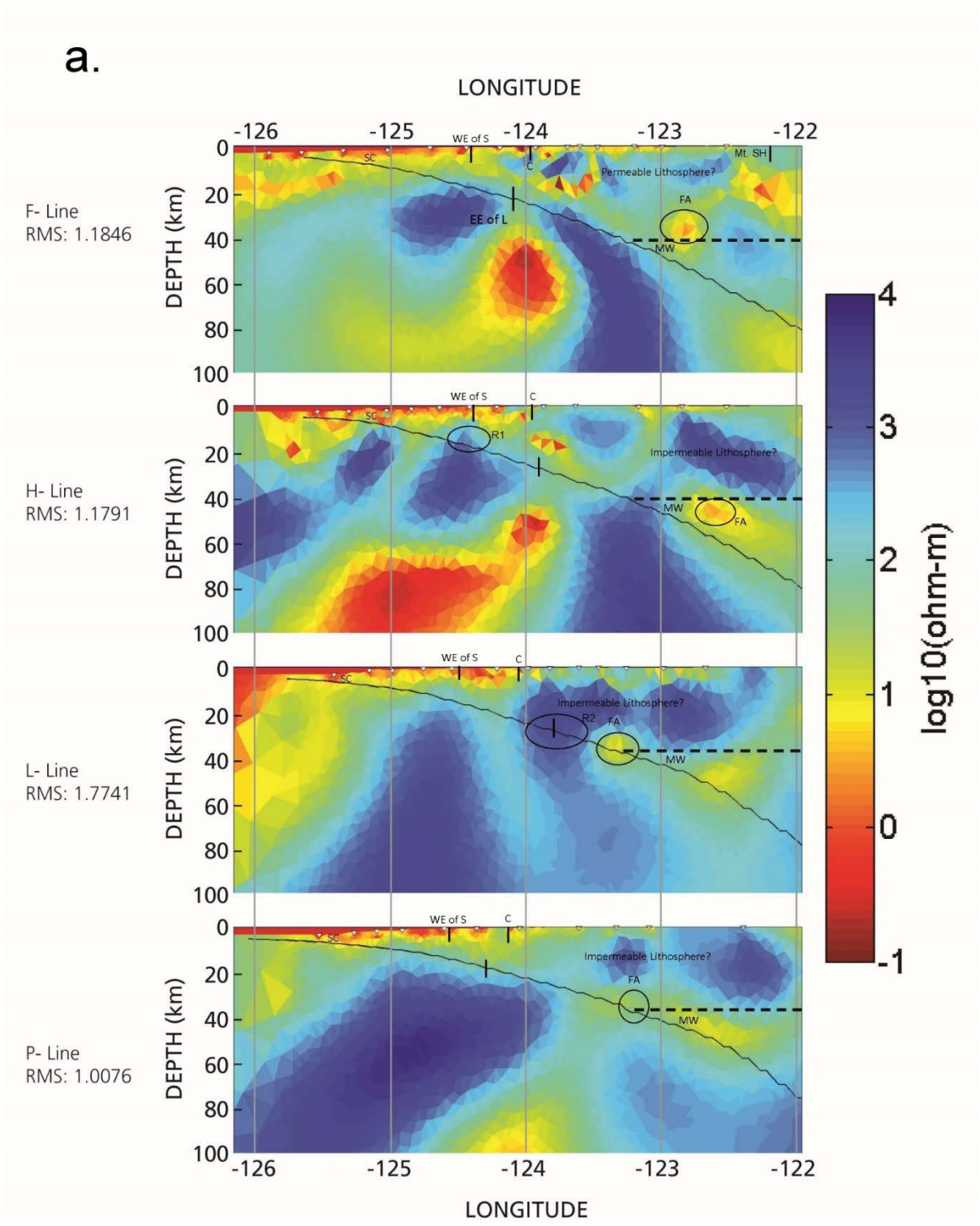
a.
LONGITUDE
-126
-125
-124
-123
-122
WE of S
C
SC
Mt. SH
Permeable Lithosphere?
FA
EE of L
MW
DEPTH (km)
0
20
40
60
80
100
F- Line
RMS: 1.1846
R1
Impermeable Lithosphere?
H- Line
RMS: 1.1791
R2
L- Line
RMS: 1.7741
P- Line
RMS: 1.0076
log10(ohm-m)
4
3
2
1
0
-1

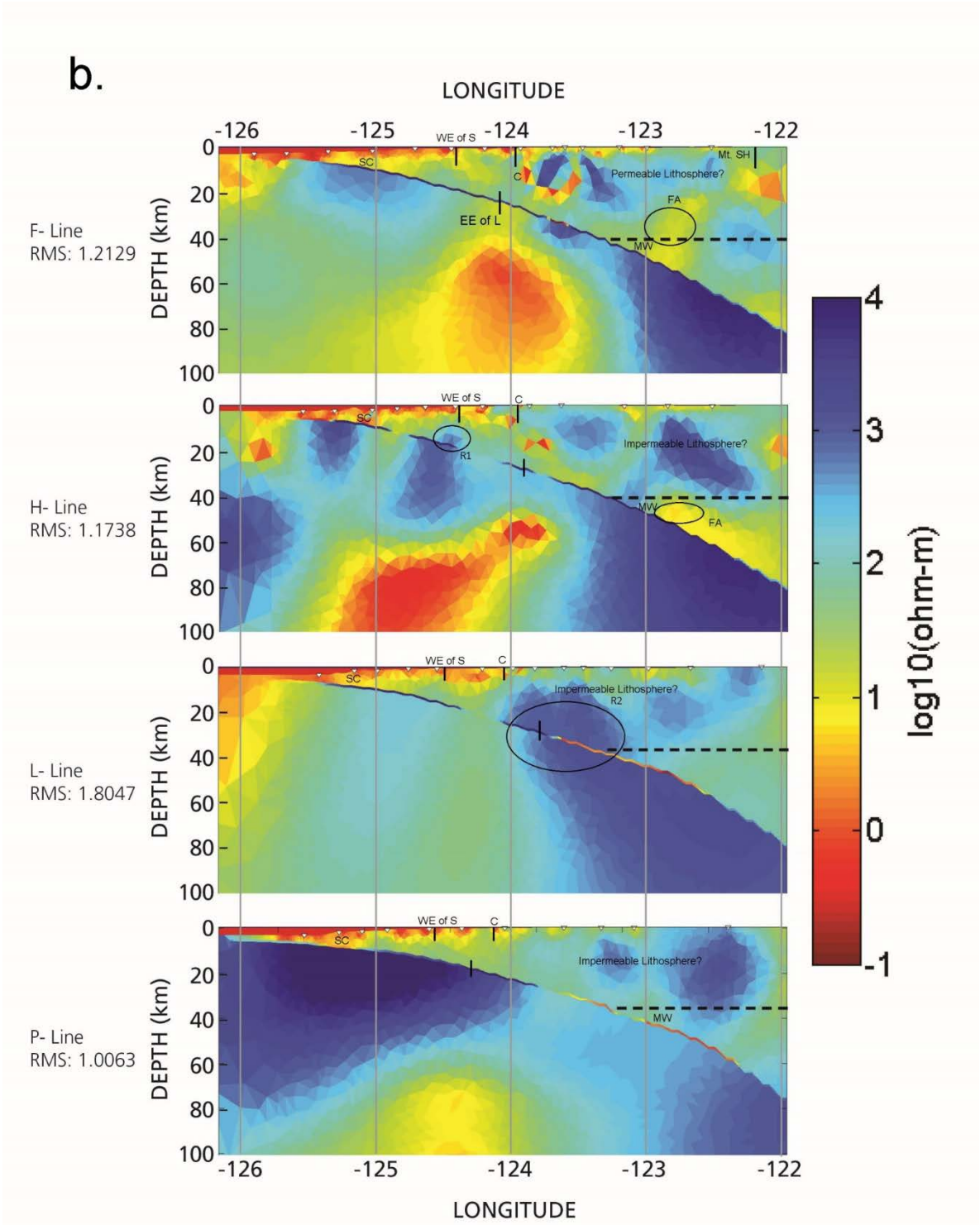
b.
LONGITUDE
-126
-125
-124
-123
-122
DEPTH (km)
0
20
40
60
80
100
WE of S
C
SC
Mt. SH
Permeable Lithosphere?
FA
EE of L
MW
F- Line
RMS: 1.2129
R1
Impermeable Lithosphere?
H- Line
RMS: 1.1738
R2
L- Line
RMS: 1.8047
P- Line
RMS: 1.0063
log10(ohm-m)
4
3
2
1
0
-1

Figure 6: Eight 2-D inversions of MOCHA data.

The models are laid out north to south (top to bottom). For their exact latitudes refer to Figure 5. Inversions in b. were inverted with the McCrory slab, whereas inversions in a. have McCrory slab[35] locations superimposed on the unconstrained model. The white triangles on the top of each model indicate MT station location. The black dashed line located at ~36 - 40 km depth depicts the Moho.[36] Vertical grey lines indicate integer lines of longitude. Abbreviations include western extent of Siletzia (WE of S), Coast (C), eastward extent of locking (EE of L)[37], mantle wedge (MW), fluid accumulation (FA), subduction channel (SC), Mount Saint Helens (Mt. SH), resistor 1 (R1), resistor (R2).

I would like to start with a discussion of the set of inversions which are simple 2-D MT inversion without implementation of constraints located at the slab interface (Figure 6a). We will first discuss conductivity features along the plate interface, starting at the mantle wedge corner and work our way up-dip to the trench. Following an analysis of the four lines, I will briefly compare my 2-D L-line inversion of MOCHA data to Wannamaker et al. 2014 inversion of EMSLAB.

Let's first analyze the features at the mantle wedge corner approximately located at 40 km depth and -123 longitude. Down-dip of the mantle wedge corner, every line images patches of low resistivity along the plate interface until ~60 km depth. This conductivity can be equated to the release of fluids from the dehydration of subducted hydrous minerals.[38] According to Furukawa 2009 hypothesis, we should see accumulation of these released fluids at the mantle wedge corner. The L and P- line shows conductors at the mantle wedge, whereas H- line and F- line show conductors just east of the wedge. This can be interpreted as the fluid accumulation that Furukawa

[35] Mccrory, Blair, Waldhauser, Oppenheimer, 2012
[36] Bostock, 2013
[37] Schmalzle, Mccaffrey, Creager, 2014
[38] Furukawa, 2009

predicted. The location of the conductors in F and H- line are not located directly on top of the indicated mantle wedge, however the location of the indicated mantle wedge is only an approximation.

This fluid accumulation seems to be nominally more conductive in the northern lines than in the southern lines; specifically, the conductivity-area product is larger in the north, suggesting larger accumulation of fluids in the north as opposed to the south. The conductivity of the North American plate directly above these features is not uniform. The F- line indicates dispersed conductivity directly overhead, and H,L, and P show much more resistive structures. The F- line is located at, or just north of the segmentation boundary of northern and central Cascadia, and H, L and P are located within central Cascadia. Recall that northern Cascadia is associated with much more frequent ETS occurrence than the central region. In the F- line, the dispersed conductivity directly above FA can be explained by a more permeable rock matrix that has allowed episodic pore pressure build up at FA to push fluids into the overlying crust. The three southern lines resistive structures above FA would then indicate an impermeable rock structure, lacking fluids, that instead contains high pore pressures promoting “partial creeping” in the ETS zone. This trend is consistent in Wannamaker et al. 2014 inversions of CAFE line which is located in the northern region of Cascadia. Wannamaker et al. interprets a conductor beginning at the mantle wedge and extending up and arc-ward as fluids penetrating the crust and originating from dehydration reactions, suggesting a more permeable crust. In summary, the higher conductivity in the overlying crust in F- line could be evidence for a permeable crust in the north, and the lower conductivity in the overlying crust in H, L and P- line could be evidence for a

less permeable overlying crust in central Cascadia. This resistivity structures at each of the mantle wedge corners and directly above each of the ETS regions in Figure 6 seems to agree with the conceptual model proposed by Schmalzle et al. 2014 and Furakawa 2009.

Up-dip of the ETS region and the eastward extent of locking (EE of L) conductors are imaged along the plate interface in both slab-constrained models (Figure 6b) and unconstrained models (6a). There are two exceptions (R1 and R2). The conductors along the plate interface are again ascribed to fluids released by dehydration of hydrous minerals subducted in the oceanic crust. These fluids are thought to be highly pressurized and trapped by the dense overriding Siletzia terrain to roughly ~35km off coast (WE of S), reducing the normal forces between the plates, and facilitating partial creep instead of strong locking.[39] Eastern, thicker, portions of Siletzia are apparent in the three southern lines, but no line images resistive western portions of thinner Siletzia expected to extend to ~35 km off coast.[40] [41] This may be an inevitability of the magnetotelluric method working in tandem with the smoothing requirements imposed for these inversions. MT is very good at finding the tops of conductors, but tends to exaggerate the extent of their depth. The westernmost portion of resistive Siletz basalt is sandwiched between a conductive sea floor, and conductive fluids lying at the plate interface. It is very likely that any resistive element in this region would be masked by the smoothing between the two conductors. In addition, MOCHA marine stations only sampled 17 longer periods, resulting in poor resolution at

[39] Schmalzle, Mccaffrey, Creager, 2014
[40] Trehu, Blakely, Williams, 2011
[41] Wannamaker et al., 2014

these shallow depths. This dense basalt is an important geological feature that could help explain the locking patterns in Cascadia, and with current data sets and my inversion techniques MT will not image this feature. One could attempt to fix a resistive element in a starting model at the location of Siletzia, and determine whether the resulting inversion would satisfy the data similarly.

There are two resistive features along the plate interface up-dip of the mantle wedge in Figures 6a and Figure 6b: one in H- line (R1) and one in L- line (R2). R1 implies lower amounts of interconnected fluids. In turn, a lack of fluids to promote low stress deformation should enable seismic energy build up. This would contradict strong geodetic evidence that locking degree is low in this region. This discrepancy may be attributed to a very thin layer of fluids along the interface that may not be sensed with the limited number of sampled periods. Further investigation of this feature is required.

A large portion of the plate interface is shown to be resistive in L- line (R2) in both sets of models. This also contradicts evidence for low locking degree in this region, and may also be explainable by the limited number of periods collected at MOCHA land stations. An alternate explanation is that this resistive structure lies at a secondary locking zone located in this region.[42] Krogstad et al. 2016 propose the possibility of a secondary locked zone located at 31 km depth at this latitude. Wanamaker et al. 2014 inversion of EMSLAB (Figure 7) images a similar but less well-defined resistive structure in the same region. There may be some relationship between the high resistivity in this region, and the presence of a secondary locked zone. As

[42] Krogstad, Schmidt, Weldon, Burgette, 2016

mentioned before, high resistivity indicates a lack of fluids which can promote seismic energy build up.

There are several features on the eastern and western extents of Figure 6a and Figure 6b that are not well constrained by MT data and thus may not be requirements of the inversion. F and H- line image strong conductors below the slab starting at 40 km - 50 km depth. Longer-period data at overlying stations indicate the presence of some conductive features at depth, but it may not be so strongly conductive, or broadly distributed. The conductor immediately below Mt. Saint Helens may be related to the volcano.

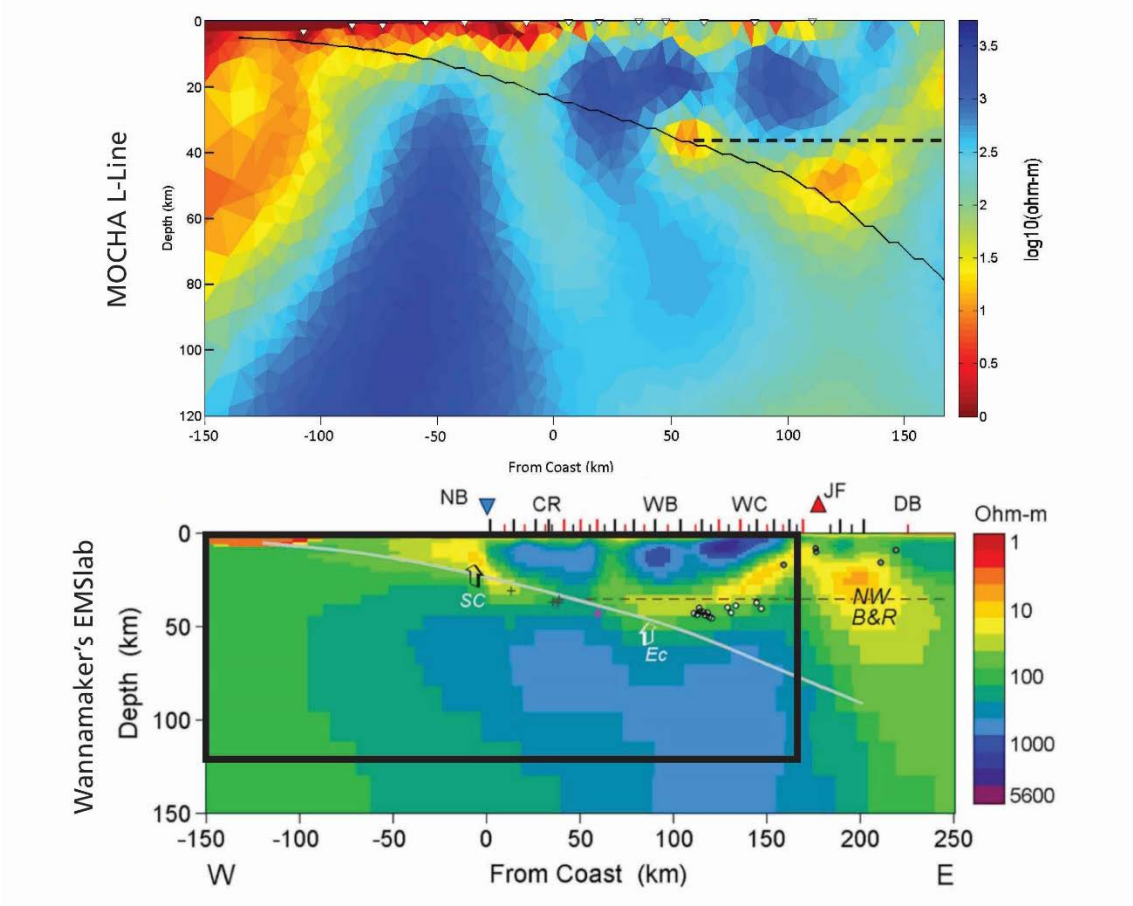

Figure 7: A comparison of L- line and Wannamaker et al. EMSLAB.

The portion of EMSLAB relevant to L- line is indicated with a black box. EMSLAB marks Newport Basin (NB), Coastal Range (CR), Willamette Basin (WB), Western Cascades (WC), Mount Jefferson (JF), Deschutes Basin (DB), Subduction channel (SC), eclogitization (EC), and north west Basin and Range (NW B&R).

Figure 7 compares Wannamaker et al.'s interpretation of EMSLAB to L- line. Despite arising from different data set, which includes higher frequency data, both models look very similar. Conductors are imaged in both models along the plate interface from the trench to the coast, and at the mantle wedge. The largest disagreement between the models in well resolved regions is along the plate interface,

from the coast to the mantle wedge. L- line images this region as very resistive, where EMSLAB images this region as decreasingly conductive.

EMSLAB and L- line are two different data sets taken more than thirty years apart, and yet inversions of these different data sets reveal similar models. This validates MOCHA data, EMSLAB data, and both 2-D inversion methods. Inversion processes used in F, H, L and P were all the same, therefore this similarity between L and EMLAB also provides some validity to the other MOCHA lines inverted.

Conclusions

Four 2-D MT inversions of Cascadia MOCHA data yield conductivity maps and thus fluid distribution variations between 43N and 46N in the Cascadia subduction zone. L- line inversion produced from MOCHA data and the nominally coincident Wannamaker et al. 2014 EMSLAB inversion have very similar conductivity structures. This similarity serves to provide some validation to L- line as well as the other MOCHA MT lines inverted. Relativity consistent conductors, interpreted as fluid, lying along the plate interface for inversions in central Cascadia fit within the hypothesis that the central region is poorly locked. These fluids, trapped by an overriding impermeable crust, serve to reduce normal forces between the plates and allow for "partial creeping." Shallower regions over the locked zone in Cascadia were not well resolved in this study due to issues with the MOCHA dataset, as well as inherent shortcomings of the MT inversion method. This suggests future work where a resistive "core" is imposed over the locked zone, representing North American Crust, and tested to see if the resulting inversion is similarly compatible with MOCHA L-line data. There may be some relationship between the high resistivity in the ETS region of L- line, and the presence of a secondary locked zone. This resistor is confined to this latitude and does not extend to the bordering northern or southern MT transects suggesting the secondary locking is localized.

Fluid accumulation was imaged in all lines at or near the mantle wedge corner, where more fluid was shown in the northern lines compared to the southern lines. The crust overlying the fluid accumulation appears to lack fluid in central Cascadia, indicating an impermeable overriding crust. The crust at the southern terminus of

northern Cascadia appears to be full of dispersed fluids indicating a permeable overriding crust. This finding may imply that a permeable crust, with more fluid at the mantle wedge can be associated with more frequent ETS. A relatively impermeable overriding lithosphere, with less fluid at the mantle wedge can be associated with less frequent ETS. These 2-D inversions have proved useful for initial interpretations of MOCHA data, but the integrity of these findings should be checked against 3-D inversions once they are well developed.

Bibliography

Audet, Pascal, Michael G. Bostock, Devin C. Boyarko, Michael R. Brudzinski, and Richard M. Allen. "Slab Morphology in the Cascadia Fore Arc and Its Relation to Episodic Tremor and Slip." *J. Geophys. Res. Journal of Geophysical Research* 115 (2010).

Audet, Pascal, and Susan Y. Schwartz. "Hydrologic Control of Forearc Strength and Seismicity in the Costa Rican Subduction Zone." *Nature Geoscience Nature Geosci* 6, no. 10 (2013): 852-55.

Bostock, M. G., R. D. Hyndman, S. Rondenay, and S. M. Peacock. "An Inverted Continental Moho and Serpentinization of the Forearc Mantle." *Nature* 417, no. 6888 (2002): 536-38.

Bostock, M.g. "The Moho in Subduction Zones." *Tectonophysics* 609 (2013): 547-57.

Brocher, Thomas M., Tom Parsons, Anne M. Tréhu, Catherine M. Snelson, and Michael A. Fisher. "Seismic Evidence for Widespread Serpentinized Forearc Upper Mantle along the Cascadia Margin." *Geol Geology* 31, no. 3 (2003): 267.

Brudzinski, Michael R., and Richard M. Allen. "Segmentation in Episodic Tremor and Slip All along Cascadia." *Geol Geology* 35, no. 10 (2007): 907.

Bürgmann, Roland. "Interseismic Coupling and Asperity Distribution along the Kamchatka Subduction Zone." *J. Geophys. Res. Journal of Geophysical Research* 110, no. B7 (2005).

"Unlocking the Cascadia Subduction Zone's Secrets: Peering into Recent Research and Findings." EARTH Magazine. http://www.earthmagazine.org/article/unlocking-cascadia-subduction-zones-secrets-peering-recent-research-and-findings.

Evans, Rob L., Philip E. Wannamaker, R. Shane Mcgary, and Jimmy Elsenbeck. "Electrical Structure of the Central Cascadia Subduction Zone: The EMSLAB Lincoln Line Revisited." *Earth and Planetary Science Letters* 402 (2014): 265-74.

Furukawa, Y. "Convergence of Aqueous Fluid at the Corner of the Mantle Wedge: Implications for a Generation Mechanism of Deep Low-frequency Earthquakes." *Tectonophysics* 469, no. 1-4 (2009): 85-92.

Krogstad, Randy D., David A. Schmidt, Ray J. Weldon, and Reed J. Burgette. "Constraints on Accumulated Strain near the ETS Zone along Cascadia." *Earth and Planetary Science Letters* 439 (2016): 109-16.

Mccrory, Patricia A., J. Luke Blair, Felix Waldhauser, and David H. Oppenheimer. "Juan De Fuca Slab Geometry and Its Relation to Wadati-Benioff Zone Seismicity." *J. Geophys. Res. Journal of Geophysical Research: Solid Earth* 117, no. B9 (2012).

Meqbel, Naser M., Gary D. Egbert, Philip E. Wannamaker, Anna Kelbert, and Adam Schultz. "Deep Electrical Resistivity Structure of the Northwestern U.S. Derived from 3-D Inversion of USArray Magnetotelluric Data." *Earth and Planetary Science Letters* 402 (2014).

Moreno, Marcos, Christian Haberland, Onno Oncken, Andreas Rietbrock, Samuel Angiboust, and Oliver Heidbach. "Locking of the Chile Subduction Zone Controlled by Fluid Pressure before the 2010 Earthquake." *Nature Geoscience Nature Geosci* 7, no. 4 (2014).

Peacock, Simon M. "Thermal and Metamorphic Environment of Subduction Zone Episodic Tremor and Slip." *J. Geophys. Res. Journal of Geophysical Research* 114 (2009).

Perfettini, Hugo, and Jean-Paul Ampuero. "Dynamics of a Velocity Strengthening Fault Region: Implications for Slow Earthquakes and Postseismic Slip." *J. Geophys. Res. Journal of Geophysical Research* 113, no. B9 (2008). doi:10.1029/2007jb005398.

Perfettini, Hugo, Jean-Philippe Avouac, Hernando Tavera, Andrew Kositsky, Jean-Mathieu Nocquet, Francis Bondoux, Mohamed Chlieh, Anthony Sladen, Laurence Audin, Daniel L. Farber, and Pierre Soler. "Seismic and Aseismic Slip on the Central Peru Megathrust." *Nature* 465, no. 7294 (2010): 78-81.

Schmalzle, Gina M., Robert Mccaffrey, and Kenneth C. Creager. "Central Cascadia Subduction Zone Creep." *Geochemistry, Geophysics, Geosystems Geochem. Geophys. Geosyst.* 15, no. 4 (2014): 1515-532.

Schulz, Kathryn. "The Really Big One." The New Yorker. 2015. http://www.newyorker.com/magazine/2015/07/20/the-really-big-one.

Song, T.-R. A. "Large Trench-Parallel Gravity Variations Predict Seismogenic Behavior in Subduction Zones." *Science* 301, no. 5633 (2003): 630-33.

Stern, R. J. "Where Are Subduction Zones?" Geology. https://www.utdallas.edu/scimathed/resources/Melville/g_wherearesubductionzones.html.

"WE WATCH: Is Japan Going to Sink?! Pt.3 - Seabed Shifted by 50 Meters (165 Feet) - the Largest Slip Yet Recorded." The Watchers. http://thewatchers.adorraeli.com/2011/12/04/we-watch-is-japan-going-to-sink-pt-3-seabed-shifted-by-50-meters165-feet-the-largest-slip-yet-recorded/.

Trehu, A. M., R. J. Blakely, and M. C. Williams. "Subducted Seamounts and Recent Earthquakes beneath the Central Cascadia Forearc." *Geology* 40, no. 2 (2011): 103-06.

Vidale, John E., and Heidi Houston. "Slow Slip: A New Kind of Earthquake." *Phys. Today Physics Today* 65, no. 1 (2012).

Vozoff, K. "Magnetotellurics: Basic Theoretical Concpets." (1972).

Wannamaker, Philip E., Rob L. Evans, Paul A. Bedrosian, Martyn J. Unsworth, Virginie Maris, and R. Shane Mcgary. "Segmentation of Plate Coupling, Fate of Subduction Fluids, and Modes of Arc Magmatism in Cascadia, Inferred from Magnetotelluric Resistivity." *Geochemistry, Geophysics, Geosystems Geochem. Geophys. Geosyst.* 15, no. 11 (2014): 4230-253.

Wikipedia. https://en.wikipedia.org/wiki/2004_Indian_Ocean_earthquake_and_tsunami#Earthquake_characteristics.